

## BepiColombo Laser Altimeter Simulator

K.U. Schreiber<sup>a</sup>, M. Hiener<sup>a</sup>, H. Michaelis<sup>b</sup>

<sup>a</sup>Forschungseinrichtung Satellitengeodaesie,  
Technische Universitaet Muenchen  
Geodaetisches Observatorium Wettzell, 93444 Bad Koetzing, Germany  
<sup>b</sup>DLR e.V. Institute of Planetary Research  
Rutherfordstr. 2, 12489 Berlin, Germany  
schreiber@fs.wettzell.de

### Abstract

*One of the payload instruments for the BepiColombo Mercury Orbiter Mission is a laser altimeter, designed for a precise mapping of the terrain of the planet Mercury. BepiColombo is projected for an elliptical polar orbit with an apogee of about 1500 km and a perigee of about 400 km. While the proximity to the sun places substantial demands on the actual laser altimeter hardware design, the elliptical orbit and the insufficient knowledge of the gravity field of Mercury provide similar challenges for the actual measurement process. Therefore we have designed and created a numerical simulation tool, which allows us to develop and study suitable procedures for the actual measurement process of the laser altimeter. Different scenarios depending on the quality of the assumed satellite orbit and the presence of a terrain of unknown topography can be studied in detail. This paper describes the software concept and the basic functions of the altimeter simulation tool.*

**Key words:** Laser Altimetry, Orbit Simulation, Laser Link Budget  
PAGS: 06.30.Gv, 42.79.Qx, 95.55.-n, 42.50.Ar

### 1. Introduction

Laser altimetry for solar system bodies, although a well established technology, contains several severe challenges. Since it constitutes a range measurement based on the travel time of short optical laser pulses [1], this range measurement is related to the center of mass of the spacecraft and hence the satellite orbit defining the origin of the measured range. The reflection from the footprint of the laser on the probed celestial body marks the end of the distance of interest, from which the topography then can be derived. A simplified form of the ranging equation therefore is

$$r = \frac{1}{2} c \Delta\tau, \quad (1)$$

with  $r$  the distance between the position of the satellite and the laser footprint on the ground,  $c$  the actual propagation velocity of light and  $\Delta\tau$  the time between the laser pulse departure and return. The factor of 1/2 accounts for the two way passage of laser pulse.

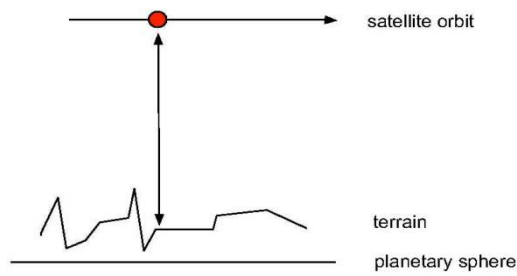


**Figure 1.** Pulse laser and detector are located on the satellite in orbit. Measuring the time of flight determines the contour of the terrain along the ground track of the satellite.

Figure 1 illustrates this concept. From a sequence of such range measurements one can eventually derive the topography of the probed celestial body along the ground track of the spacecraft. There are several ways in which such an altimeter can be operated. In accordance with the BepiColombo laser altimeter [5] we restrict ourselves to a fixed nadir pointing instrument, but the whole concept could also be extended to a sideways pointing or swath scanning sensor. When a suitable orbit is chosen a high percentage of the entire planetary surface can be mapped throughout the satellite mission. While orbit uncertainties may generate errors for the topographic mapping, they also cause difficulties during the measurement process in particular when a high background light level is present and techniques like receiver gating are required. The BepiColombo mission to Mercury is such an example [5].

In this paper we want to introduce and discuss a simulation program, which allows the investigation of the impact of orbit errors, unknown terrain variations and general system parameters on the shot by shot altimetry measurement [6]. Depending on a predefined orbit, the altimeter hardware layout and an arbitrary user supplied planetary topography the simulation program evaluates the signal link budget for each laser shot. So it is possible to test various hardware and flight configurations as well as a variety of ground return recovery strategies and to explore their limitations.

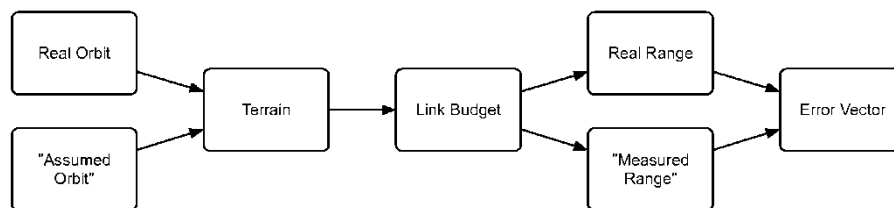


**Figure 2.** Flow chart of the simulation program.

## 2. Simulator Concept

The simulator is constructed from several subsystems. Figure 2 outlines the flow chart of the entire program. In order to study the influence of orbit uncertainties with respect to the data recovery strategy, the system generates two different orbits during the initialization of the

program. One of the orbits is the actual orbit used during the simulation run for the echo signal computation, while the other orbit corresponds to the one 'assumed' by the onboard range prediction and measurement processor. Both orbits are specified by the user at startup time. When they differ from each other, one can study the level of robustness of the echo identification and data acquisition procedure. The specific functions of the simulator are discussed below.

### 2.1. Satellite Orbit and Groundtrack

In order to simulate altimeter function the program first computes an unperturbed Keplerian orbit according to user supplied orbital parameters. Once the orbit is computed, the radius of the celestial body is used to establish the distance between the orbiter and the spherical body. In the next step a topographic structure is added to the object. This elevation model is also user provided and can be scaled in horizontal and vertical direction in order to test different scenarios. As a default configuration we have inserted a topographic map of central Europe into the program, because the alpine region provides substantial changes in the terrain profile. In order to study a more realistic scenario, textures of other solar system bodies may also be supplied by specifying a data-file where the topographic information is contained in a tabular form. Apart from using the entire terrain, the user is free to select a portion of interest. Figure 3 shows the default terrain as an example. While the figure displays the entire currently available surface structure, the highlighted area shows a subset with larger variations in topographic height. Sections like this can be selected from the simulation program during the setup phase to facilitate specific studies.

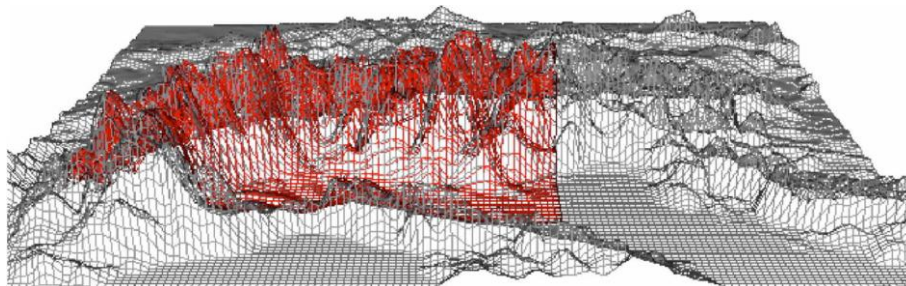


**Figure 3.** Central Europe as an example for a terrain profile used in the simulation process.

### 2.2. Laser Altimeter Parameters

The link budget for an orbiting altimeter can be calculated from a number of essential hardware and geometrical parameters [2]. Apart from the actual transmitter and receiver design, the range, terrain albedo and roughness, background optical radiation and attenuation along the path of signal propagation are important.

Table 1 summarizes the currently available transmitter parameters on the left side and quantifies the settings used for the examples in this paper. In a similar way one can define the system characteristics for the receiver part of the laser altimeter. They are shown on the right hand side of the table. Variable mission related parameters like the shot by shot range are obtained from the orbit calculation, while other mission related constant settings are also adjustable in the parameter panel. Table 2 shows the available items. The solar background radiation in tab. 2 can be switched on and off altogether in order to investigate the differences between a measurement in daylight or at nighttime. Since the parameter settings panel can be

viewed and altered at any time throughout the entire simulation run, it displays the instantaneous range and the angle of incidence of the laser beam on the planet surface as a result of the chosen topographic features.

**Table 1.** Available transmitter and receiver parameters for the simulator and their respective settings used throughout this paper

Transmitter		Receiver	
Wavelength:	1.064 $\mu\text{m}$	Detection Sampling Freq.:	200 MHz
Pulse Energy:	10000 $\mu\text{J}$	Noise equivalent Power:	$3 \times 10^{-14} \frac{\text{W}}{\sqrt{\text{Hz}}}$
Pulse Width (FWHM):	6 ns	Detector Quant. Eff.:	0.4
Beam Div. (full angle):	00 $\mu\text{rad}$	Spectral Filter Bandw.:	0.2 nm
Telescope Diameter:	0.25 m	Receive Optics Transm.:	0.7
Pulse Repetition Freq.:	0.02 kHz	Field of View (full angle):	200 $\mu\text{rad}$
		Detection Gatewidth:	20 $\mu\text{s}$

**Table 2.** Mission related adjustable parameters

Mission Parameters
Surface Albedo: 0.26
Surface Roughness: 1 m (rms)
Solar Background radiation: 432.3 $\text{W}/\text{m}^2\text{sr}\mu\text{m}$

### 2.3. Link Budget Calculation

Once the orbits are calculated and the altimeter and mission parameters are set up, the simulator loops either through an entire revolution of the satellite around the planet or through a user selected shorter segment of interest on a shot by shot basis. Depending on the repetition rate of the laser, the satellite is advanced along the 'true' orbit and the distance between the actual position and the planet surface including the terrain structure is computed. The intensity and temporal dispersion of the return signal is then calculated based on the hardware settings of the parameter panel. The program computes the return signal level for a nadir pointing instrument according to the general altimeter equation [3]

$$n_{pe} = \eta_q \eta_t \left( \frac{E_t}{h\nu} \right) \eta_r \left( \frac{A_r}{\pi r^2} \right) \frac{\beta}{\Omega_g}, \quad (2)$$

where  $n_{pe}$  is the number of detected photo-electrons,  $\eta_q$  the detector quantum efficiency,  $\eta_t$  the transmit path transmission,  $E_t/h\nu$  the number of generated photons at the laser output,  $\eta_r$  is the receive path transmission,  $A_r$  the effective receive telescope area,  $r$  the distance between altimeter and ground,  $\beta$  the surface albedo and  $\Omega_g$  the scattering angle of the surface ( $\pi$  steradian). For simplicity we assume a nadir pointing instrument ( $\theta = 0$ ) and that there is no atmosphere for the light to pass through. Otherwise  $\beta$  has a  $\cos(\theta)$  dependence (assuming a surface with Lambertian scattering) and we would have to include additional signal attenuation to account for atmospheric absorption and scatter. In order to compute the signal

response as seen by the photo detector the signal broadening due to the surface roughness across the laser footprint and the width of the laser pulse has to be incorporated. We assume a Gaussian distribution for the signal spread in time for both signal broadening processes.

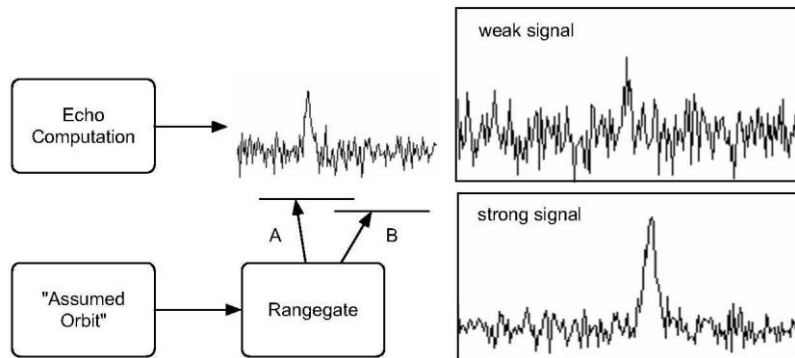


**Figure 4.** Example of the signal representation of the simulation program for a correctly and an incorrectly placed detector gate. Typical return signals with good and poor signal to noise ratio are also shown.

This part of the simulation program corresponds to true physical modeling section of the measurement process. From the 'assumed' orbit, which in this simulation corresponds to the best a priori knowledge of the true orbit and the epoch of the laser fire event a range-gate window of predefined length is computed. This time interval is filled with the appropriate level of background noise, which a real photodetector would have seen under these experimental conditions. In the next step the temporal structure of the computed return signal is inserted into the synthetic detector signal in the time domain. When the 'assumed' and the 'real' orbit are close enough and the range-gate is not too short, the simulated ground echo actually fits into the signal representation of the range-gate. This corresponds to case A in fig. 4. If the generated signal and the range-gate are too far apart in time, case B in fig. 4 applies and there is no echo signal contained in the synthetic range-gate. Since the altimeter and orbital parameters may vary substantially, the signal strength and shape of the ground response can also change over a wide dynamic range. Figure 4 (right side) gives two such examples to illustrate this variability, which outlines the importance of a suitable echo identification procedure.

#### 2.4. Range-gate Generation

In the current version the simulation program uses the assumed orbit reduced by a 'best guess' predefined value to account for the expected terrain profile when it calculates the roundtrip time of the laser pulse. When the laser pulse is fired it opens the range-gate by a user specified offset time (typically around 20  $\mu\text{s}$ ) prior to the calculated return epoch and closes the range-gate after a similar delay past the expected echo event. After the range-gate is closed the entire measurement window is scanned for a valid return event. When a ground echo is identified within the gate, the offset from the center is determined and used as an additional correction for the prediction of the next laser shot. In this way it is possible to track the variation of the terrain with the receiver range-gate. After three consecutive successful datations, the gate module narrows the range-gate down to 500 m  $\approx$  1.5  $\mu\text{s}$  in order to guard the detector from over loading due to the strong background radiation flux typical for Mercury. When the ground return is accidentally lost in the range window, the simulator

widens the window up again and the identification process restarts. Figure 5 shows the simulated ground echo for a low signal to noise ratio (SNR). One can see the full preset gatewidth corresponding to the initial operating situation in fig. 5a. The gatewidth reduces from 40  $\mu\text{s}$  to less than 2  $\mu\text{s}$  after 3 consecutive consistent signal detections in the wide gate as shown in fig. 5b. A short measurement gate speeds the echo detection process significantly up, reduces the probability of false alarms and lost datations and protects the photo-detector from excess signal loads. For the case of good SNR the respective signals are shown in fig. 6a and b. Comparing the two different observation cases, one can see that the altimeter controlling program needs to optimize operations for two operational parameters, namely low SNR and a proper range-gate tracking. Furthermore it is important to note how far the actual echo may be offset from the initially calculated distance in the large detection gates, when the assumed orbits and the terrain assumptions differ from the actual situation. This offset is adjusted shot by shot when the simulator switches over to the shorter gates.

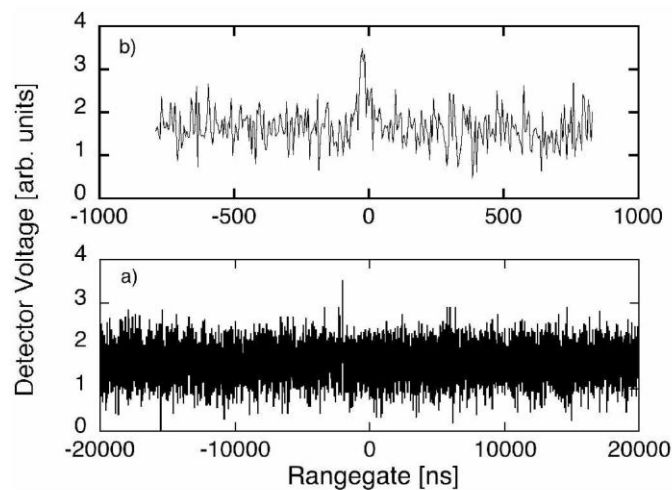


**Figure 5.** Simulated ground echo at a low signal to noise ratio for a large range-gate a) and the reduced gatewidth b).

## 2.5. Echo Signal Evaluation

The evaluation of the computed photo electric current as a function of time across the entire length of the range-gate is carried out in the next step of the simulation loop. This serves several purposes, which are

- identification of the ground return and timing the moment of detection
- finding the location of the return with respect to the opening time of the range-gate and readjusting the range-gate opening time for the return to be in the center of the next gate
- adjustment of the length of the range-gate for smallest reasonable size and high probability of an echo detection on the next shot

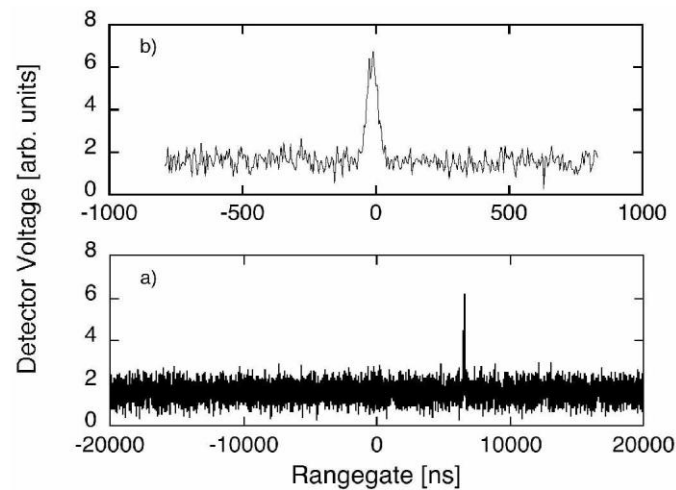


**Figure 6.** Simulated ground echo at a high signal to noise ratio for a large range-gate a) and the reduced gatewidth b).

So far, two different detection criteria have been implemented. The most common one is the threshold detection, which accepts the tallest signal peak within the range-gate as a return signal, provided the amplitude exceeds a predefined threshold. This method requires a reasonable SNR of two or more in order to be reliable. The other mechanism evaluates the width of the recorded echo. While noise contributions are usually transient events with rapid variations in amplitude (high bandwidth), ground echoes exhibit a much wider dispersion. If the laser pulse width (FWHM) is 6 ns and the rms surface roughness does not exceed a depth of 1 m, one may expect a detector pulse width of the order 4.5 ns, which is usually well discernable from noise only events even at a marginal SNR (fig. 5). The design of the simulation program is open to implement and investigate the applicability of any other signal recovery method such as Bayesian methods for example [4], in order to improve the detection probability. For the future we intend to add a combination of the threshold and the pulsewidth detection scheme as well as a correlation approach for low signal levels where the range-gate signal is correlated against a synthetic ground echo. The simulation program in general is designed to open the possibility to evaluate and compare entirely different data acquisition schemes for future missions such like the application of pulse trains in combination with the above mentioned correlation technique. New data evaluation methods can be added with little effort as user selectable subroutines in the echo detection parser loop.

## 2.6. Terrain Recovery

As the simulation program starts, it integrates the assumed satellite orbit or a selected section of it in order to obtain the satellite position for the next laser shot. Then it performs the link budget calculation and generates the respective detector signal, which in turn is analysed by the laser echo recovery procedure. This obtained range value is then subtracted from the 'actual' range value, which is computed from the 'real' orbit and the planet's surface contour. The resultant residual is interpreted as the range error value of the particular laser shot and the minimum of this value is the figure of merit of the range simulation in progress. The following properties of a laser altimeter can be studied in this way:

- Altimeter hardware design and properties
- Orbit precision requirements

- Signal recovery strategies
- Terrain slope recovery
- Laser link margins (e.g. for elliptical orbits)
- Background radiation (differences between night and day)

While the current orbit model is too simple to account for the effect of small perturbations and the current terrain is rather a one dimensional pattern, which repeats on a neighboring track when the available terrain spread is exceeded, there is no fundamental limitation that would prevent future model refinements to include spatial variations of the gravity field and eventually would allow the complete simulation of an altimeter mission including the full analysis with the aid of repeat cycles and crossover point alignments. Figure 7 shows an example of a simulated ground track. The parameter settings of the satellite passage over a rather variable terrain are listed in tab. 1. The simulations were carried out at an orbital height of around 800 km. There are 300 seconds worth of data plotted, taken at a simulated measurement rate of 10 Hz. This accumulates to a total of 3000 data points at a signal to noise ratio of about 4, similar to a return signal as shown in fig. 6.

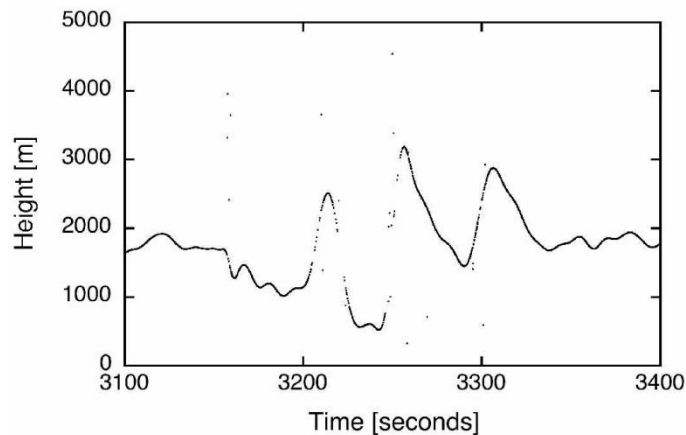


**Figure 7.** A simulated ground track for given parameterset (tab. 1) of the altimeter hardware. The track corresponds to a satellite height of 800 km.

Where the signal was reflected off from a steeply sloped terrain the experienced pulse broadening caused a reduction in signal amplitude, such that several data points were lost because the detected echo did not exceed the detection threshold value. The nevertheless seemingly rather smooth terrain variations are because of an interpolation between terrain grid points at 7 km separation. Since this gridspacing can be scaled during the initialization of the simulation program a much more rapid variation of the terrain could be examined if needed. Apart from some rare drop-outs where the rate of change exceeded the width of the small gate ( $\Delta r \geq 1$  km/s) the topography could also be recovered without problem. However the recovery rate reduces substantially when the SNR drops to values below 2. Figure 8 shows such an example. As the altitude of the satellite increases from 530 km to 740 km, more and more false readings appear in the data file. However one can still recover the ground track without problems since the percentage of false readings is still well below the 10% level.

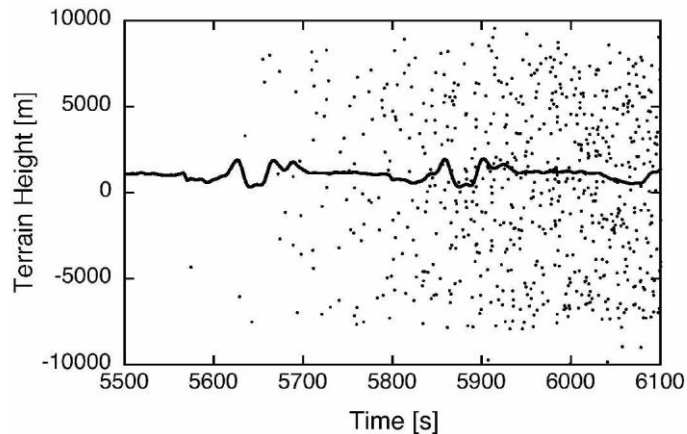
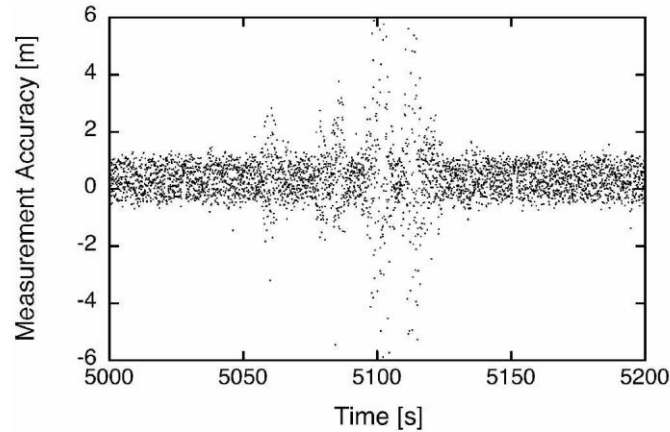


**Figure 8.** A simulated ground track for a signal to noise ratio below two. The corresponding orbital height went from 530 to 740 km.

### 3. Error Vector

For a laser repetition rate below 20 Hz and reasonable signal levels the simulation program runs roughly in real time on a standard office computer and Labview<sup>1</sup> version 8.2. However for a low return signal level requiring frequent switching between a large and a narrow range gate, the necessary time to complete a loop of simulation may go up by an order of magnitude. On the front panel of the simulation program there are a number of different diagrams available, which allow the investigation of the laser altimeter behavior and settings of the simulation in progress. At any time throughout the computation the user has full access to the altimeter parameter settings list and all values can be adjusted without the interruption of the program. All changes take effect from one shot to the next. While the shot by shot display of the range-gate content is the most educational diagram during the simulation run, other parameters like orbit distance, terrain contour recovery rate, the shot by shot deviation between the 'observed' and 'true' range (error vector) and the actually obtained pulse width are also summarized in individual charts. At the end of the simulation a data file containing the shot by shot record of the epoch of the measurement, the residual of 'true' range minus 'detected' range as well as the 'assumed' range minus the 'detected' range, the 'detected' range, the evaluated pulse width, the slope of the terrain in degrees and the slope induced dispersion of the laser pulse is written. The epoch relates to the initial point of the orbit integration and is arbitrarily chosen in the simulator. Figure 9 shows a small section of the time series of the residuals from the difference of the 'recovered' range and the 'true' range from the detector signal evaluation process. Since there was a reasonable SNR, the simulated measurement could reproduce the actually used range to within the boundaries of the specified sensor properties (pulse width, terrain roughness). The apparently blurry patches in the middle of the diagram are caused by steep terrain slopes, which increases the laser pulse spreading. As a result of this signal broadening the SNR reduces substantially and the measurement noise goes up accordingly.

<sup>1</sup>Manufacturer: National Instruments Inc.



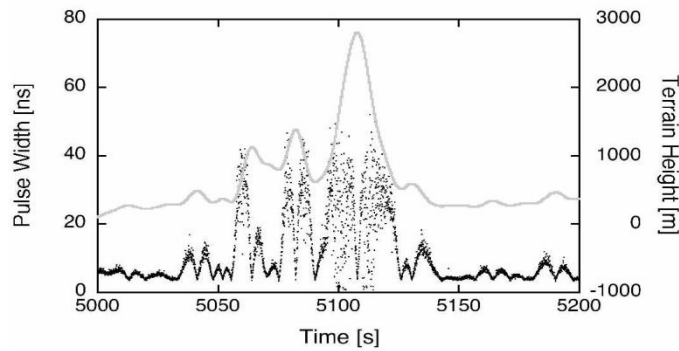
**Figure 9.** Time series of the error value of the 'recovered' range minus the 'true' range from the detector signal evaluation process. One can clearly see how steep slopes in the terrain reduce the measurement resolution by broadening the received signal pulse and reducing the SNR.

Figure 10 demonstrates this effect more clearly. For the same data section as shown in fig. 9 we have visualized the model terrain profile superimposed on the estimated return signal pulse width. While the terrain profile is shown in gray and slightly offset for better visibility, the laser pulse width was estimated by fitting a Gaussian to the 'detected' time domain voltage of the return signal. The result is displayed shot by shot in black dots. As expected the pulse width shows a minimum when the terrain slope approaches zero. This can be observed for mountain tops, valley bottoms and featureless areas. For a laser pulse width of 6 ns and a surface roughness of 1 m (rms), we obtain the expected minimum values which slightly exceeds 4 ns.<sup>2</sup> As one can see even very small contours in the ground profile reflect themselves in the laser pulse width. For extreme situations like the approximately 2500 m high mountain peak one can see that the pulse width estimates become very noisy. This is because of a substantial reduction in the signal to noise ratio, which is a consequence of the spreading of the laser pulse in the time domain. Therefore these areas coincide with areas of reduced measurement accuracy as shown in fig. 9.

#### 4. Impact of Orbit Errors

In order to evaluate the robustness of the range recovery algorithm a test run was performed, where both the assumed and the real orbit were equal, however with a bias for the time of 2 seconds between them. As a result one obtains a rapidly changing range offset of several hundred meter, accumulating to nearly 1 km over a section of 1000 seconds around the perigee of the elliptical orbit. Although the model errors for the radial distance variations are substantial, the resulting 1 m/s range offsets can be accommodated and tracked by the adaptive range-gate routine of the simulator without problem.

<sup>2</sup>The actual value is divided by 2 because of the two-way passage of the simulated laser beam



**Figure 10.** Time series of the estimated shot by shot pulse width of the return signal beam (black dots) superimposed on the corresponding terrain profile (gray line) for the same data section as fig. 9. One can see that the pulse width is a very sensitive measurement quantity for the terrain slope. Even small changes in terrain reflect themselves strongly in the pulse width.

Figure 11 shows a graphical representation for this example. However the resultant cumulative orbit error will place high demands on to the initial ground echo acquisition process, because the difference between the predicted (assumed) and the actually existent (real) range may differ by more than a kilometer. For a case of good SNR one will obtain ground echos within a few shots, but for weak signals in particular for a situation with a high variation of the topography the initial ground echo identification process may be much more difficult. It has been one of the major goals of this simulator project to provide a tool, where suitable data acquisition approaches can be developed and verified over a wide range of anticipated operational conditions.

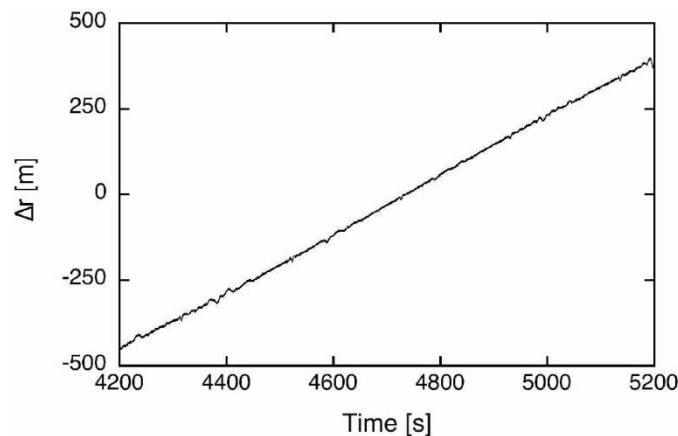


**Figure 11.** Time series of the error value of the 'true' range and the 'recovered' range from the detector signal evaluation process. The apparently discrete nature of this value is a result of the limited bandwidth of the sampling rate.

## 5. Conclusion

We have developed a flexible simulation program for spaceborne laser altimeter applications. The laser link budget and the structure of a ground echo in the time domain for a pulsed laser

with a Gaussian profile is calculated over a terrain of user specified roughness and topography on a shot by shot basis. A special feature of the simulation program is a clear separation between the physical model of the laser echo at the instantaneous satellite position and the echo recovery procedure, which works on a different set of orbital parameters. In this way one can not only test the signal response and echo recovery of the modeled altimeter design, but also test and optimize the control program algorithms and the influence of orbit uncertainties on the data recovery and signal identification. So far we have included basic test functions like an unperturbed Keplerian orbit around a spherical celestial body, a user defined terrain structure and two methods of ground echo recovery (threshold and pulsewidth detection). Parameters like current range, recovered terrain profile, pulse spreading of the ground echo and the difference value between the distance defined by the physical model and the distance obtained by the 'measurement' are continuously available for inspection throughout the simulation run. A datafile with a time series of the simulation results is generated at the end of a program run. It is intended to further develop this simulation program by adding more modules for echo reconstruction techniques, which will allow a higher and more robust echo identification rate at lower return signal levels. At the moment we can only analyse the terrain profile along the satellite ground track. If required, future versions of this simulator may be extend to also allow the reconstruction of a complete surface topography.

## Acknowledgement

The work presented in this paper is based on the study LAPE-DLR-BG-3000-012 (Laser Altimeter for Planetary Exploration) carried out by DLR and partners in 2003. The authors acknowledge discussions and contributions of I.Leike and J.Oberst. KUS and MH acknowledge the support through an internal DLR grant.

## References

- [1] Degnan, J. J.; *"Millimeter Accuracy Satellite Laser Ranging: A Review"*; Contributions of space geodesy to geodynamics: technology, (AGU Publication Vol. 25), DE Smith and DL Turcotte editors, ISBN: 0-87590-526-9, 133 - 181, (1993)
- [2] ESA study report; *"BepiColombo: An Interdisciplinary Cornerstone Mission to the Planet Mercury"*; ESA-SCI(2000)1, (2000)
- [3] Gardner C.S.; *"Ranging Performance of satellite laser altimeters"*; Proc. IEEE **30**, (5), 1061 - 1072, (1992)
- [4] Luthcke, S.B., Rowlands, D.D., McCarthy, J.J., Pavlis, D.E., Stoneking, E.; *"Spaceborne laser-altimeter-pointing bias calibration from range residual analysis"*; J. Spacecraft Rockets **37**, (3), 374 - 384, (2000)
- [5] Thomas, N., Spohn, T., Barriot, J.-P., Benz, W., Beutler, G., Christensen, U., Dehant, V., Fallnich, C., Giardini, D., Groussin, O., Gunderson, K., Hauber, E., Hilchenbach, M., Iess, L., Lamy, P., Lara, L.-M. Lognonne, P., Lopez-Moreno, J.J., Michaelis, H., Oberst, J., Resendes, D., Reynaud, J.-L., Rodrigo, R., Sasaki, S., Seiferlein, K., Wiczorek, M., Whitby, J.; *"The BepiColombo Laser Altimeter (BELA): Concept and baseline design"*; Planetary and Space Science **55**, 1398 - 1413, (2007)
- [6] Zuber, M.T., Smith, D.E., Solomon, S.C., Abshire, J.B., AFZAL, RS., Aharonson, O., Fishbaugh, K., Ford, P.J., Frey, F.V., Garvin, J.B., Head, J.W., Ivanov, A.B., Johnson, C.L., Muhleman, D.O., Neumann, G.A., Pettengill, G.H., Phillips, RJ., Sun, X.,

Zwally, H.J., Banerdt, W.B., Duxbury, T.C.; *"Observations of the North Polar Region of Mars from the Mars Orbiter Laser Altimeter"*; Science, **282**, 2053 - 2060, (1998)